J Mater Sci: Mater Med (2011) 22:1231–1246
DOI 10.1007/s10856-011-4285-8

Physicochemical characterisation and biological evaluation of polyvinylpyrrolidone-iodine engineered polyurethane (Tecoflex®)

Anand P. Khandwekar · Mukesh Doble

Received: 18 October 2010 / Accepted: 8 March 2011 / Published online: 25 March 2011
© Springer Science+Business Media, LLC 2011

Abstract Bacterial adhesion and encrustation are the known causes for obstruction or blockage of urethral catheters and ureteral stents, which often hinders their effective use within the urinary tract. In this in vitro study, polyvinylpyrrolidone-iodine (PVP-I) complex modified polyurethane (Tecoflex®) systems were created by physically entrapping the modifying species during the reversible swelling of the polymer surface region. The presence of the PVP-I molecules on this surfaces were verified by ATR-FTIR, AFM and SEM-EDAX analysis, while wettability of the films was investigated by water contact angle measurements. The modified surfaces were investigated for its suitability as a urinary tract biomaterial by comparing its lubricity and ability to resist bacterial adherence and encrustation with that of base polyurethane. The PVP-I modified polyurethane showed a nanopatterned surface topography and was highly hydrophilic and more lubricious than control polyurethane. Adherence of both the gram positive *Staphylococcus aureus* (by 86%; $^{**}P < 0.01$) and gram-negative *Pseudomonas aeruginosa* (by 80%; $^{*}P < 0.05$) was significantly reduced on the modified surfaces. The deposition of struvite and hydroxyapatite the major components of urinary tract encrustations were significantly less on PVP-I modified polyurethane as compared to base polyurethane, especially reduction in hydroxyapatite encrustation was particularly marked. These results demonstrated that the PVP-I entrapment process can be applied on polyurethane in order to reduce/lower complications associated with bacterial adhesion and deposition of encrustation on polyurethanes.

Electronic supplementary material The online version of this article (doi:10.1007/s10856-011-4285-8) contains supplementary material, which is available to authorized users.

A. P. Khandwekar · M. Doble (✉)
Department of Biotechnology, Indian Institute of Technology Madras, Chennai 600036, India
e-mail: mukeshd@iitm.ac.in

1 Introduction

Urinary medical devices have been employed for the treatment of various urological conditions, including incontinence, obstructive uropathy, primary or malignant carcinomas, radiation fibrosis or retroperitoneal fibrosis [1, 2]. Indwelling ureteral stents and urethral catheters are synthetic polymeric biomaterials used extensively in the upper and lower urinary tract, respectively, to facilitate urine drainage. The most commonly used materials in the manufacture of urological devices are silicone, latex, polyvinylchloride and polyurethanes or polyurethane-based polymers. Unfortunately, whilst these polymeric devices represent a major advance in urology, their use is still associated with several clinical problems, including fracture [4–6], encrustation [7] and infection [8, 9]. In particular, medical device-related infections are frequently associated with morbidity and, more importantly, mortality and therefore represent a serious clinical problem [2, 8]. Adherence of microorganisms to medical devices represents the initial step in the development of biomaterial centered infections (BCI). Following this, the bacteria may exude and become encased within an exopolymeric material, referred to as the biofilm. Within the biofilm, the bacteria exhibit greater resistance to antimicrobial agents. Furthermore, bacteria may become dislodged from the biofilm and initiate an infection in the adjacent region.

Whilst the consequences of BCI have been well documented, e.g. [1–8], the clinical consequences of encrustation and particularly, infection based encrustation should

not be overlooked. In particular, infection blockage of urine flow and possible degradation of the biomaterial are frequently associated with clinical encrustation. Urological implants are frequently affected by encrustation due to their permanent contact with urine. Crystals and deposits consisting of the ionic and organic components of urine cover the surface of the implant [10]. The formation of encrustation deposits is promoted by a high urinary pH, the product of infections. Encrustation leads to a higher risk of infection, and a vicious circle begins [11]. Thus, the encrustation of urological implants does not only cause their failure by obstructing the lumen [12, 13], but it also presents a focus for infection [14]. Thus the development of bacterial biofilm and encrustation [15] of urological implants that leads to obstruction of urine flow with attendant discomfort for the patient [16] is as yet an unresolved problem and requires an urgent solution.

Amongst the currently used polymers for urinary applications including latex, silicone, polyvinylchloride and polyurethane, discernable differences have been reported in their resistance to encrustation and infection [15, 16]. Traditionally latex was used to manufacture these implants. More recently silicone and polyurethanes have been employed as they are relatively inert at the biomaterial/tissue interface and has superior biomechanical properties. Of all these polymeric materials silicon has been shown to be more resistant to bacterial adhesion and encrustation than other biomaterials [26]. Several studies have also shown that none of the polymeric biomaterials presently used in the urinary tract are capable of resisting bacterial adherence [1–8] and encrustation [10–14] in vitro. Attempts have been made to produce biomaterials which resist bacterial adhesion and encrustation, yet at the same time are biocompatible and have physical properties rendering them suitable to their function. To improve their resistance, there have been reports in which these conventional materials have been coated with coatings such as hydrogels [17, 18] or Teflon [17] to increase their lubricity and make the material easy to insert and comfortable to the patient. Although in the past Teflon has been used to improve the lubricity, however, there is now a body of evidence which suggests that conventional Teflon coatings promote several bacterial interactions [1, 2]. Hydrogels are hydrophilic polymeric networks that represent another class of material that has found extensive use as coatings of urinary medical devices. These biomaterials are biocompatible, the high equilibrium water content of the material rendering it soft, lubricious and pliable like natural tissue [19]. In this respect, the application of hydrophilic hydrogel coatings which render the material surface unattractive to bacteria and encrusting deposits may be particularly beneficial. Previous studies have examined the use of such coatings applied to a range of implanted medical devices [23–28]. Hedelin and Grenabo [20] reported that hydrogel-coated latex exhibited lower encrustation than silicone-coated latex in synthetic urine, whereas Liedberg et al. [21] described the resistance of hydrogels containing silver ions to encrustation. Similarly, hydrogel-coated urinary tract devices have also been shown to reduce adherence of bacteria. However, many of these coatings have proved to be relatively ineffective and indeed, in a recent comparative study of five commercially available materials (silicone, Siliteks, polyurethane, Percuflexs and a hydrogel-coated polyurethane), Tunney et al. [15] reported that (uncoated) silicone exhibited maximum resistance to infections and encrustation. However, more recently, the ability of a hydrogel-coated biomaterial, Aquavenes, to resist encrustation was reported by the same authors [22], validating the potential clinical usefulness of polymeric coatings on urological biomaterials.

A need therefore exists, for the development of polymeric biomaterials that are able to resist bacterial adherence and encrustation. Tecoflex® an aliphatic polyether urethane has been chosen as a model substrate in this study since it has extensive applications in a variety of biomedical devices (including urological devices). Previously, we reported a surface entrapment technique as an effective strategy for surface modification of biomedical polymers such as polyurethane, poly(ethylene terepthalate), poly(methylmethacrylate) and poly(caprolactone) [28–34]. In present study, Tecoflex® surface was engineered with polyvinylpyrrolidone-iodine complex by surface entrapment during the reversible swelling of the polymer surface region. The entrapment technique followed in the present work does not involve any toxic reagents but uses only aqueous solutions and also follows mild reaction conditions. Surface changes after the modification process was extensively probed with several spectroscopic and microscopic analytical techniques. Thus the objectives of this work were to investigate the suitability of PVP-I modified polyurethane for use as a urinary tract biomaterial by comparing its lubricity, ability to resist bacterial adhesion/biofilm formation (Gram-positive *S. aureus* and Gram-negative *P. aeruginosa*) and encrustation development.

2 Materials and methods

2.1 Surface entrapment process

Tecoflex® (EG-93A-B40) was obtained in the form of granules as a gift from Devon Innovations, Bangalore (India). A 50 mg/ml solution in tetrahydrofuran (Merck) was used to cast films of 1.5 mm wet thickness using a casting knife. These films were cured for 6 h in an oven at 60°C to evaporate the solvent.

To determine the optimal conditions for surface engineering of PU, we quantified the entrapment of fluorescently tagged dextran (Dextran-Rhodamine, Sigma) on PU. It was found that a 45% v/v dilution of THF was optimal for surface entrapment process (Figs. S1 and S2). The surface modifying solution was then prepared by first dissolving Polyvinylpyrrolidone-Iodine complex (Acros organics, UK) in deionized filtered water (DIFW), and then adding tetrahydrofuran to it. The resultant mixture consisted of 5% w/v of PVP-I and 45% v/v of THF. Tecoflex® (PU) films were immersed in 10 ml of this solvent/nonsolvent mixture, following this the solution was then rapidly quenched with an excess of nonsolvent (~20 ml DIFW) and the treated films were transferred to water for storage. Exposure of the polymer to THF in the absence of macromolecules results in much faster polymer–solvent interaction, and therefore an estimation of the equivalent treatment time (as determined visually) that creates the same degree of surface swelling was used as a control to account for possible residual solvent effects on cell behavior. The films were then transferred to DIFW for storage with the water being changed periodically.

2.2 Surface characterization

Surface characterization was performed with various spectroscopic and microscopic analytical techniques as mentioned below. Hereby, for convenience PVP-I modified polyurethane will be abbreviated as PU/PVP-I respectively.

2.2.1 *Attenuated total reflection-fourier transform infrared spectroscopy*

ATR-FTIR spectra of the samples were determined using an FT/IR-4200 (Jasco, Netherlands) spectrometer having a baseline horizontal ATR accessory. Films were pressed against Zn-Se crystal, and the spectra were collected at a resolution of 4 cm^{-1} in the range of 400–4000 cm^{-1}.

2.2.2 *Atomic force microscopy*

The nanotopology of the base and the modified substrates were probed by atomic force microscopy (AFM) (Nanoscope IV, Vecco, USA). All measurements were carried out in contact mode with dry samples. A cantilever with scan rate of 2.99 Hz was used in all the experiments. Each AFM topographic image is a representative region of at least three samples and is highly reproducible under the same procedures of sample preparation. The root-mean square roughness of each image was determined with the AFM software (Veeco, USA).

2.2.3 *Scanning electron microscopy and energy dispersive X-ray analysis*

Energy dispersive X-ray analysis was performed to identify and quantify the elemental composition on the surfaces with the help of a JEOL Scanning electron microscope (Model JSM 6380, Japan). The surfaces were coated with a thin layer of platinum and the micrographs were taken at a secondary electron imaging mode, at 20 keV beam acceleration voltage with analysis time of 100 s. The ZAF program, which does not require the presence of any internal standard, was used to calculate the elemental composition of the surface [35, 36].

2.2.4 *Scanning electron microscopy investigation of the entrapment structure*

To characterize the surface structure of entrapped PVP-I molecules on surface of PU films, the specimen was investigated using a scanning electron microscope (JEOL JSM 6380, Japan). Images were collected as a stack of 2-dimensional optical sections by digitizing sequential series of images while focusing down through the specimen [31, 32].

2.2.5 *Dynamic contact-angle, surface energy and in vitro stability of surface films*

The hydrophobicity and heterogeneity of the polymer surfaces were determined by advancing and receding contact angle measurements using a Kruss Easy drop goniometer (KRUSS, DSA II GmbH, Germany). Ultrapure water was used as the contact angle liquid, and the measurements were carried out on at least five independent specimens. The surface energy of the polymer samples were calculated by the DSA2 software using Fowkes's method [37], based on contact angle measurements using three probe liquids, namely diiodomethane, formamide and water (Ultrapure). The total surface energy of a solid, γ_s, can be expressed as the sum of contributions from dispersion γ_s^d and polar γ_s^p force components on the polymer. These can be determined from the contact angle (θ) measured with the standard polar and non polar liquids by the following equation:

$$\gamma_{lv}(1+\cos\theta) = 2\sqrt{\gamma_s^d+\gamma_{lv}^d} + 2\sqrt{\gamma_s^p+\gamma_{lv}^p}$$

where γ_{lv} is the surface tension of the probing liquid, while γ_{lv}^d and γ_{lv}^p are the dispersive and polar components respectively of the surface energy of the probing liquid.

The stability of the entrapped species on the polymer substrates was determined using a previously described ultrasonication method [38]. Polymer films were dried and

subsequently their static contact angles were measured. The films were then sonicated for 3 min followed by their contact angle measurements. This cycle was repeated after gaps of 1 h each, during which period the films were equilibrated with DIFW at 37°C. The variation in water contact angle with the number of sonication cycles was monitored, which was taken as a measure of the stability of the entrapped species on the modified films. The measurements were carried out on at least five independent specimens and the average values were reported as means ± SD.

2.2.6 *Quantification of surface-immobilized PVP-I complex*

The amount of PVP-I immobilized on the surface was quantified using UV–Visible spectroscopy [39, 40]. The amount of PVP-I immobilized was monitored by recording UV–visible spectra of 1 ml of the treatment solvent as used for the surface entrapment process (containing PVP-I) taken before and after equilibration of the PU film. The polymer samples were equilibrated for a fixed time period with the treatment solution containing a known amount of PVP-I, and change in characteristic absorbance of PVP-I_2 complex at 365 nm was monitored. To convert O.D values to PVP-I surface density, a calibration curve was created with measurements from known concentrations of soluble PVP-I.

2.2.7 *Measurement of biomaterial lubricity*

The lubricity of biomaterial sections hydrated for either 10 min (five sections) or 30 min (five sections) was measured using a modification of the method described by Marmieri et al. [41]. In brief, a 7 cm section of the biomaterials to be tested were inserted parallel to the long axis of a McCartney bottle, previously filled with bacteriological agar (1% w/v, Sigma). After a period of 10 and 30 min, to allow equilibration of the interfacial layers, the samples were pulled out of the agar using a nylon thread attached to a 20 g weight. The time taken to pull the biomaterial section out of the agar was subsequently recorded as the experimentally measurable variable, the longer the time, the greater the friction at the sample/agar interface.

2.3 Bacterial adhesion studies

The two key organisms that are associated with implant related infections are gram-positive *Staphylococcus aureus* (NCIM 5021) and gram-negative *Pseudomonas aeruginosa* (NCIM 5029), so a quantitative short term adhesion (4 h) of these two bacterial species was assessed. Hundred milliliters of nutrient broth (Himedia, India) was inoculated with a single colony of bacteria from a tryptone soya agar (Himedia, India) stock plate. The broth was incubated at 37°C overnight in a shaking incubator and was split between two falcon tubes and centrifuged at 3,500 rpm for 20 min. Cells were resuspended in phosphate buffered saline. This was repeated twice more and the cells were finally resuspended at a concentration of 1×10^8 cells/ml. Three discs of each polymer were placed in a 24 well plate and were incubated in 1 ml of the cell suspension for 4 h at 37°C in a shaking incubator and rinsed twice with PBS. The bacterial cells were eluted from the surfaces into 2 ml sterile PBS using an ultrasonic cleaner (Cole-Parmer, USA). The procedure involved 4 min sonication followed by 1 min mild vortexing (repeated three times). A known volume of the sample was inoculated into Tryptone Soya agar and incubated at 37°C for 24 h. The colony forming units were counted which was an indication of the total number of bacteria retained on the surface. Statistical significance was ascertained by Student's *t* test. Similarly, bacterial adhesion on Polyurethane (Tecoflex®) stents was also evaluated. Effects of bacterial adhesion and biofilm formation of *Staphylococcus aureus* and *Pseudomonas aeruginosa* on Polyurethae(Tecoflex®) stents was also evaluated by a qualitative bacterial accumulation assay. Briefly, six stent sections (size 1 cm length) of each polymer were placed in a 24 well plate and were incubated in 1 ml of the cell suspension of 1×10^8 cells/ml for 4 h at 37°C in a shaking incubator. The samples were removed after 4 h, following the incubation time, the stent samples were rinsed once with sterile PBS. The bacteria on the stents were fixed by placement in 2.5% glutaraldehyde (v/v) in 0.1 m cacodylate buffer for 2 h. The samples were then dried with ethanol steps—50% aqueous ethanol (v/v) for 15 min, 75% aqueous ethanol (v/v) for 15 min, 95% aqueous ethanol (v/v) for 15 min and 100% aqueous ethanol (v/v) for 15 min. The biomaterials were then sputter coated with platinum using a Polaroan SC150 sputter coater and examined using a JEOL Scanning electron microscope (Model JSM 6380/FEI Quanta 200).

2.4 Encrustation development

Ten sections (size 1 cm^2) of each biomaterial were suspended in an artificial urine model and encrusted by a method as described by Tunney et al. [42, 43]. It has been shown that the encrustation produced using this model is similar to that produced in vivo and is primarily composed of the magnesium salt, struvite ($NH_4MgPO_4 \cdot 0.6H_2O$), and the calcium salt, hydroxyapatite ($Ca_{10}(PO4)_6 \cdot H_2O$) [42]. The composition of the artificial urine is shown in Table 1. The artificial urine was changed on a daily basis and to simulate conditions in the urinary tract, it was maintained

Table 1 Composition of artificial urine

Solution	Component	%w/v
A	Potassium dihydrogen ortho-phosphate	(0.76%)
	Magnesium chloride hexahydrate	(0.36%)
	Urea	(1.60%)
B	Calcium Chloride hexahydrate	(0.53%)
	Chicken ovalbumin	(0.20%)
	Urease (Jack bean urease Type IX)	(0.12%)

at a temperature of 37°C and in an atmosphere equilibrated with 5% CO_2. Five sections of each biomaterial were removed after periods of 1 and 2 weeks, rinsed gently in deionised water to remove threads of albumin before quantifying their elemental composition using Energy dispersive X-ray analysis (EDAX). EDAX analysis was performed to gain information regarding both elemental quantification and distribution/mapping of the encrustation components. Samples for EDAX were mounted on specimen stubs, coated using high vacuum carbon evaporation and examined using a FEI Quanta 200 super probe. Elemental analysis of the encrusted deposits allowed comparison by individual element concentration, which was then converted into DIGIMAP colour-enhanced 3-D images showing the calcium, magnesium and phosphorus distributions on the materials [43].

3 Results

3.1 ATR-FTIR analysis

The ATR-FTIR spectrum of the PU/PVP-I film was notably different from the virgin PU film in the regions 1298, 1662, 1540, and 3450 cm^{-1} (Fig. 1). The strong peak at 1298 cm^{-1} in the PU/PVP-I films apparently corresponded to the stretching ν(C–N) amide III, vibrations and peaks in the 1400–1500 and 2850–3000 cm^{-1} region possibly to plane deformational vibrations of the CH and CH_2 stretches from the chain and the pyrrolidone rings [44]. The I.R spectrum of PU/PVP-I also showed appearance of a new carbonyl stretching peak at 1662 cm^{-1} region which was not visible on the bare PU surface. This peak is a mixed mode containing contributions from the C=O (amide II) stretching and N–C stretching vibrations of PVP-I molecules in PU/PVP-I films [45, 46]. The broad peak around 3452 cm^{-1} is related to amide N–H stretches [44, 45]. Thus, the ATR-FTIR spectrum indicated chemical structural changes in the PU/PVP-I surface as compared to the bare PU indicating successful immobilization.

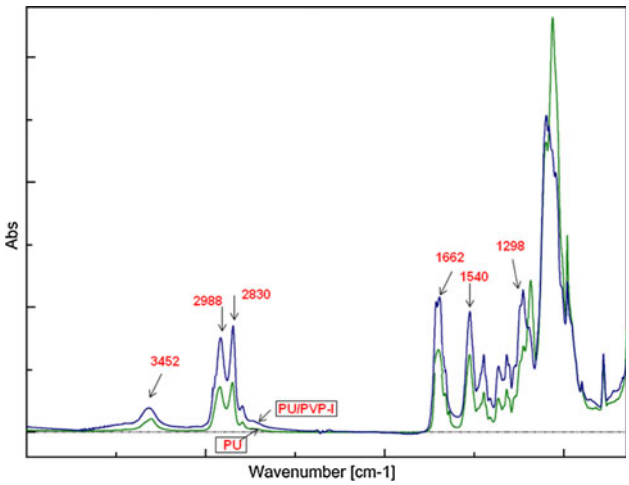

Fig. 1 ATR-FTIR spectra of unmodified and PVP-I modified polyurethane films

3.2 Atomic force microscopy analysis

AFM studies were aimed at visualizing the nanostructural changes in the surface topology before and after modification. Both two-dimensional (2D) and three-dimensional (3D) views of PU surface before and after modification with PVP-I are shown in Fig. 2. Quantitative measurement of surface microrugosity (Rq) revealed PU surface was relatively smooth at the atomic level with RMS roughness of 9.226 nm (Fig. 2a), while entrapment of PVP-I complex on the surface of PU marginally increased the RMS roughness to 19.384 nm (Fig. 2b). Further topographic investigation of the surfaces using section analysis revealed that the PU surface lacked major surface features (Fig. 2c), while immobilization of PVP-I complex resulted in surface showing nanoscale ridges and furrows with typical nanopatterned topographical features (Fig. 2d). Thus, the AFM analysis indicated changes in the surface topography, with the PU-PVP-I surface showing characteristic nanopatterned topography.

3.3 SEM-EDAX analysis

The changes in the elemental composition of the surface upon modification were also investigated by SEM-EDAX, which provided insight into the microscopic composition. The surface elemental composition and the calculated N/C ratios of the modified and unmodified PU films as estimated by SEM-EDAX are shown in Table 2. The spectra of base PU showed peaks for carbon, oxygen and nitrogen, whereas the PU/PVP-I showed an additional peak for the presence of iodine. There was a significant increase in the N/C ratio upon immobilization of PVP-I molecules. Thus, SEM-EDAX results also indicated that PVP-I has been successfully immobilized onto PU surface.

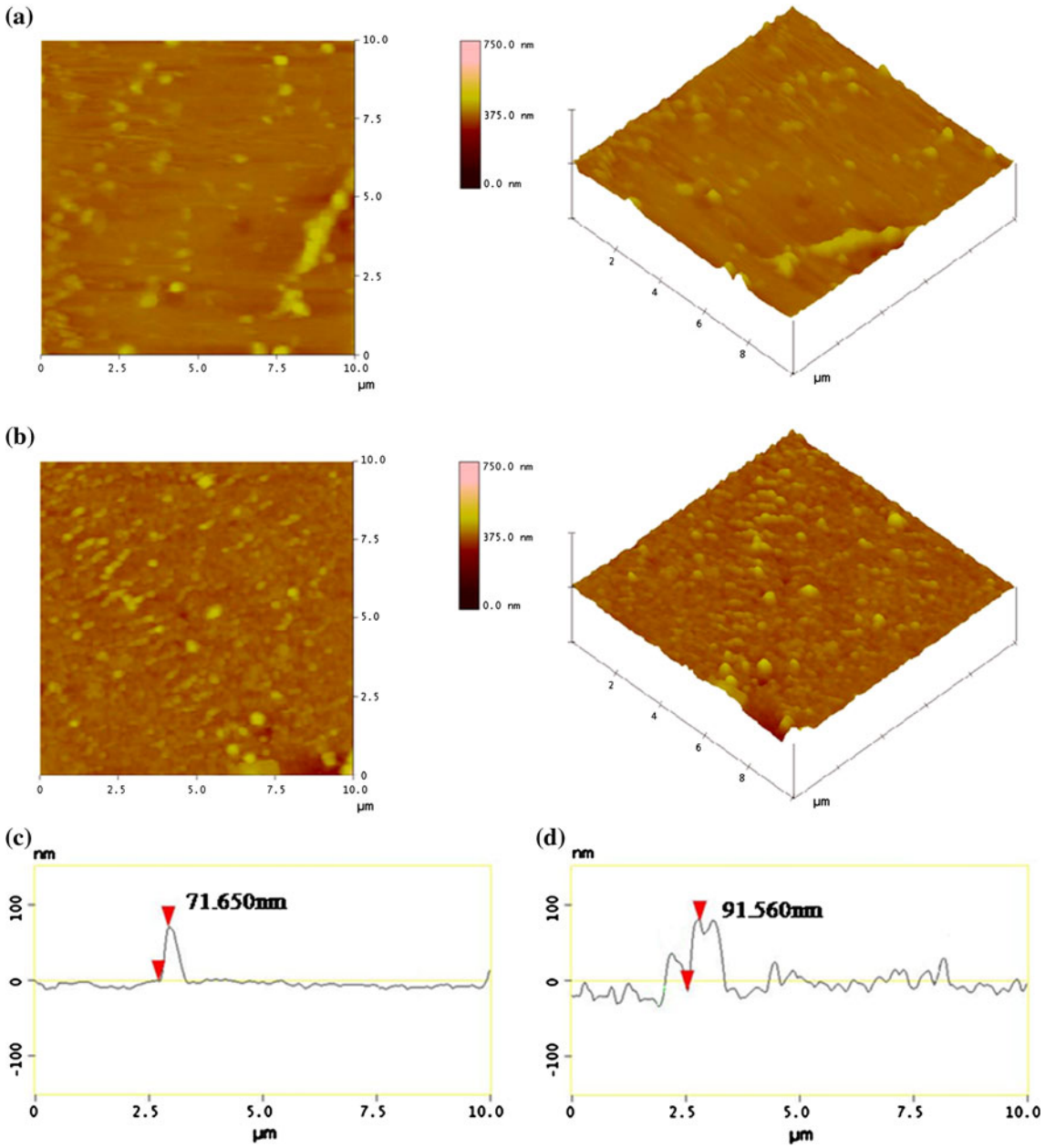

Fig. 2 Typical AFM topographic images of **a** PU and **b** PU/PVP-I films. Section analysis of **c** PU and **d** PU/PVP-I surfaces

Table 2 Surface elemental composition of the various polyurethane films by EDAX

Sample	Weight percent (%)				
	C	N	O	I	N/C
PU	33.07	25.45	11.30	–	0.79
PU-PVPI	26.72	33.71	8.15	32.42	1.26

3.4 Scanning electron microscopy investigation of entrapment structure

The cross-sectional part of the PU/PVP-I film is shown in (Fig. 3a and b). It can be seen in the figures that both sides of the PU/PVP-I film were uniformly covered with PVP-I molecules. The thickness of the entrapped PVP-I layer was determined using the SEM

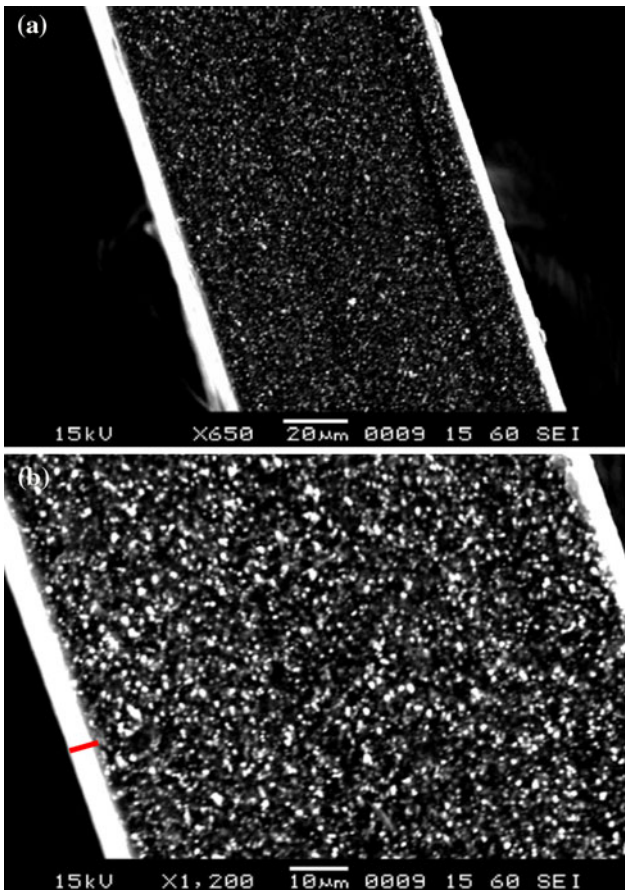

Fig. 3 Scanning electron microscopy investigation of cross-section part of the entrapment film. SEM image of cross-section of a polyvinylpyrrolidone-iodine complex entrapped PU film

Table 3 Dynamic contact angle analysis of various polyurethane films

Polymer	Advancing contact angle (θ_A)	Receding contact angle (θ_R)	Hysterisis ($\theta_A - \theta_R$)
PU	91.4° ± 2.2	84.2° ± 1.3	7.2°
PU-THF	86.5 ± 2.0	79.0 ± 1.8	7.5°
PU/PVP-I	46.4 ± 3.0	22.65° ± 4.0	23.7°

scale from Fig. 3b and was found to be approximately 10–12 µm.

3.5 Dynamic contact-angle, surface energy and in vitro stability of surface films

The PU surface exhibited a typical hydrophobic nature characterized by relatively high values of advancing ($\theta_A = 91.4°$) and receding contact angles ($\theta_R = 84.2$) (Table 3). Immobilization of PVP-I complex rendered the surfaces more hydrophilic, which was seen by reduction in the values of both θ_A and θ_R. The PU/PVP-I surface showed much higher hysteresis, indicating that on hydration reorientation of hydrophilic PVP-I chains occurs on the surface of PU/PVP-I leading to even more hydrophilic and wetted surface as compared to bare PU.

Table 4 Surface free energy and their components of the investigated polyurethane surfaces

Sample	Dispersion component (γd) mN/m	Polar component (γp) mN/m	Surface energy (γ) mN/m
PU	23.6	8.83	32.43
PU/PVP-I	19.42	23.97	43.39

The total surface free energies and their dispersive and polar components were calculated according to the Fowkes's method and are presented in Table 4. Overall, surface free energy of the PU/PVP-I films showed an increase when compared to the base PU. The polar (γ^p) component of the surface free energy significantly increased for PU/PVP-I films compared to base PU. In other words, the modified films were more hydrophilic than original films.

The stability of PU/PVP-I films was determined by ultrasonication method. Physically adsorbed PVP-I on PU surface (PU/PVP-I/PA) is extremely unstable (Fig. 4) as a result of which it gets dislodged within the first sonication cycle, and the contact angle of this films increases to the base level (which is very similar to the bare PU surface). In contrast, the water contact angles of PVP-I entrapped film remains at nearly constant value (around 48 ± 2°) even after four sonication cycles which indicates that the PVP-I molecules are firmly entrapped and are stable on the surface.

3.6 Quantification of surface-immobilized PVP-I complex

The amount of PVP-I incorporated on the surface of PU/PVP-I films as measured by UV–visible spectroscopy, was around 90 ± 4 µg/cm^2 respectively.

3.7 Measurement of biomaterial lubricity

Measurement of the length of time required to remove the biomaterial sections from agar revealed significant differences in the lubricity of the biomaterial surfaces (Fig. 5). Removal of PU from the agar required mean times of 7 and 21 s following hydration for 10 and 30 min, respectively. Surface modification of PU with PVP-I molecules rendered the PU/PVP-I surfaces more lubricious, with mean times of only 6 and 8 s required to remove the PU/PVP-I from the agar after 10 and 30 min hydration, respectively.

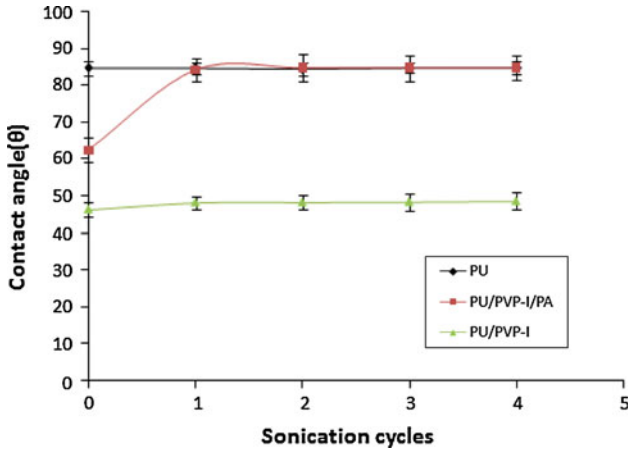

Fig. 4 Stability of the PVP-I modified PU films. Water contact angles vs. sonication cycles

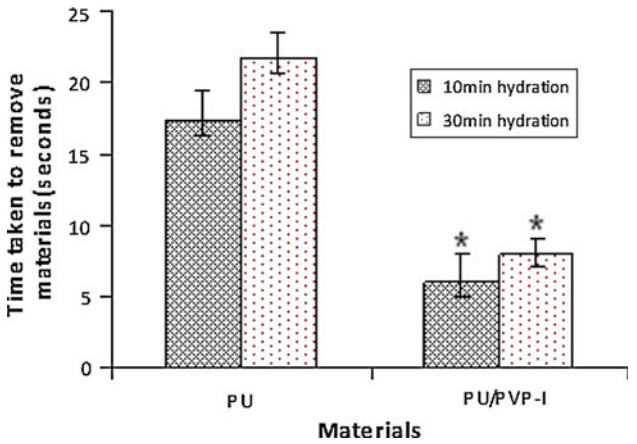

Fig. 5 Time taken to remove biomaterials from bacteriological agar. Values represent means ± SD from ten measurements (*$P < 0.05$; $n = 10$)

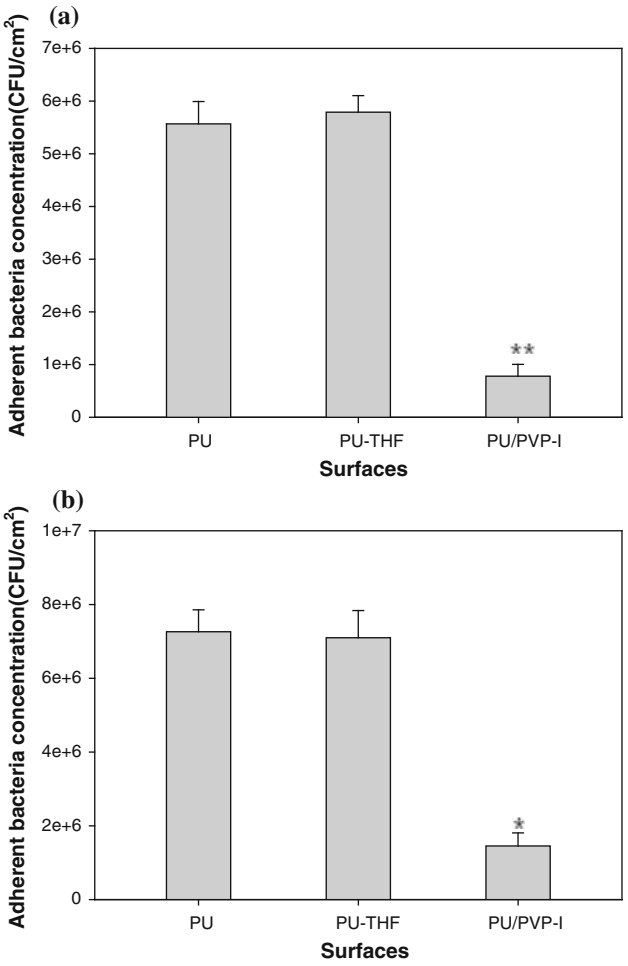

Fig. 6 Bacterial adhesion on materials incubated in approximately 1×10^8 cells/ml **a** *S. aureus* and **b** *P. aeruginosa* after 4 h. Values represent means ± SD from a single experiment performed in triplicates, which was representative of three independent experiments ($n = 3$ in each group; **$P < 0.01$; *$P < 0.05$)

3.8 Bacterial adhesion studies

Statistical analysis indicated that there was no significant reduction in adhesion of both the *Staphylococcus aureus* and *Pseudomonas aeruginosa* species between untreated PU and control PU-THF ($P > 0.05$). But, PU/PVP-I surface significantly reduced adhesion of both *Staphylococcus aureus* (Figs. 6a and 7b, **$P < 0.01$) and *Pseudomonas aeruginosa* (Figs. 6b and 7d; *$P < 0.05$) after 4 h, when compared to PU and PU-THF control. Although the extent of reduction was found to be greater for *Staphylococcus aureus* (86%) when compared to *Pseudomonas aeruginosa* (80%). The cross-sections of polyurethane (Tecoflex®) stents were observed using SEM along the length of the stents. Results for all the six stents of each polymer were observed and the representative pictures are shown in Figs. 8 and 9. Figure 8 shows representative qualitative images of accumulated *S. aureus* on bare PU, and PU/PVP-I stent surfaces. In these growth mode experiments, less biofilm accumulation was observed qualitatively on PU/PVP-I stents after 4 h period. Whereas the hydrophobic bare PU surface exhibited higher accumulation of *S. aureus*.

Similar differences were also observed in the accumulation of *P. aeruginosa* as shown in Fig. 9. The bare PU surface exhibited higher accumulation of the bacteria, while in contrast the bacterial accumulation on PU/PVP-I stent was drastically reduced.

3.9 Encrustation development

Low-power SEM of the PU/PVP-I surface after 2 weeks of encrustation revealed that the surface was only partially covered by encrusting deposits (Fig. 10c and d). In contrast, the PU surface was almost completely covered with

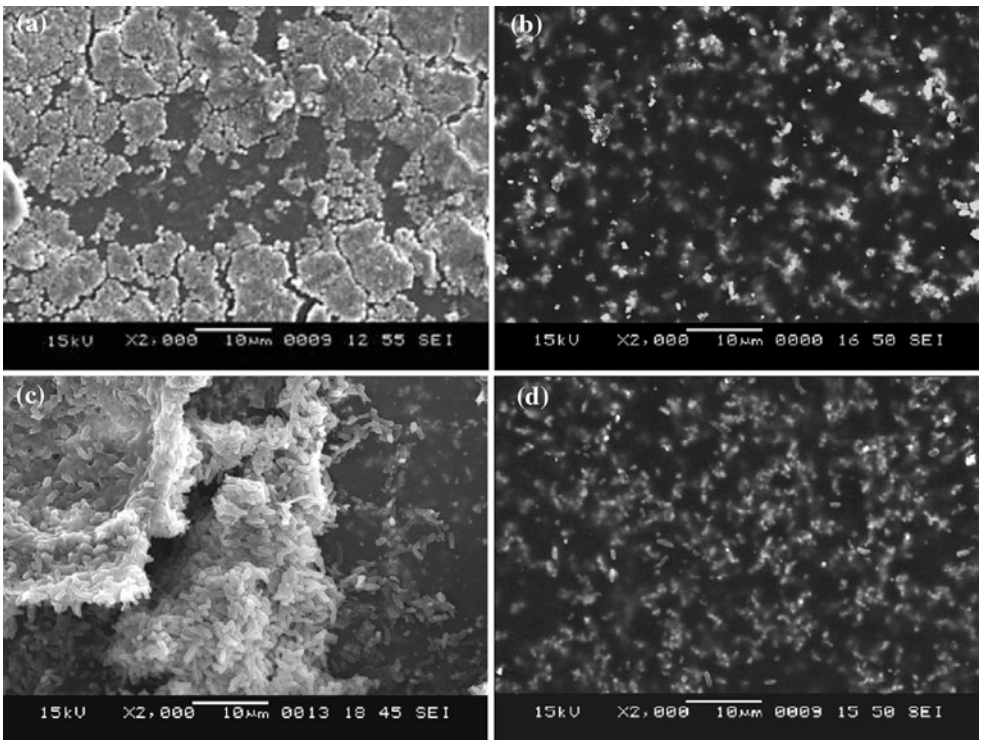

Fig. 7 Reprehensive scanning electron microscopic images of *S. aureus* (**a**, **b**) and *P. aeruginosa* (**c**, **d**) adhesion on PU (**a**, **c**) and PU/PVP-I (**b**, **d**) surfaces after 4 h

encrusting deposits at this time (Fig. 10a and b). Further examination at a higher magnification revealed the presence of both large column-like struvite crystals and smaller hydroxyapatite crystals on the PU surface (Fig. 10e). In order to detect and analyze low level invisible crystalline deposits, quantitative EDAX-analysis was performed. In the case of the control PU after 1 week of encrustation, the $K_{\alpha 1}$-lines of calcium, magnesium and phosphorus are clearly resolved as are also, to smaller extent, the $K_{\beta 1}$-lines of these elements (Fig. 11a), whereas the spectrum of PU/PVP-I showed no pronounced peaks for calcium, magnesium and phosphorous (Fig. 11b). This confirmed the presence of considerable amounts of phosphorus, magnesium and calcium, the main components of encrustations, on PU surface. Statistical analysis of the data showed that the amount of phosphorous, magnesium and calcium deposited on the PU/PVP-I surface, as determined by SEM-EDAX investigations, was significantly less as compared to PU (Fig. S4). A comparison of the individual element distributions of calcium, magnesium and phosphorus on the materials was made after 2 weeks using EDAX mapping (Fig. 12). This mapping experiments also revealed the complete coverage of the PU surface with calcium, magnesium and phosphorous, while PU/PVP-I surface showed partial coverage of these elements.

4 Discussion

The ability of uropathogens to adhere to the surface of biomaterials is recognized as a mechanism in the initiation and pathogenesis of infection. Within hours, adherent bacteria can aggregate and become enclosed in a protective glycocalyx to form a microbial biofilm which then becomes resistant to antimicrobial therapy and host defences [37, 38]. Colonization of a biomaterial surface with urea-splitting bacteria also causes alkalinisation of the urine, which lowers the solubility of struvite and hydroxyapatite allowing them to become deposited on the biomaterial. These encrusting deposits may cause blockage of urine flow with associated pain and distress to the patients. In addition, bacteria within the biofilm matrix may be responsible for recurrent episodes of bacteruria that may lead to sepsis and fever [39]. SEM studies have shown bacterial colonies in close association with encrusting materials on ureteral catheters [40, 41] and ureteral stents [42]. For a biomaterial, therefore, to be effective at resisting encrustation it should be able to resist bacterial adherence and subsequent biofilm formation. Unfortunately, none of the biomaterials presently used for ureteral stent fabrication are capable of resisting bacterial adherence and encrustation [40–42] in vitro.

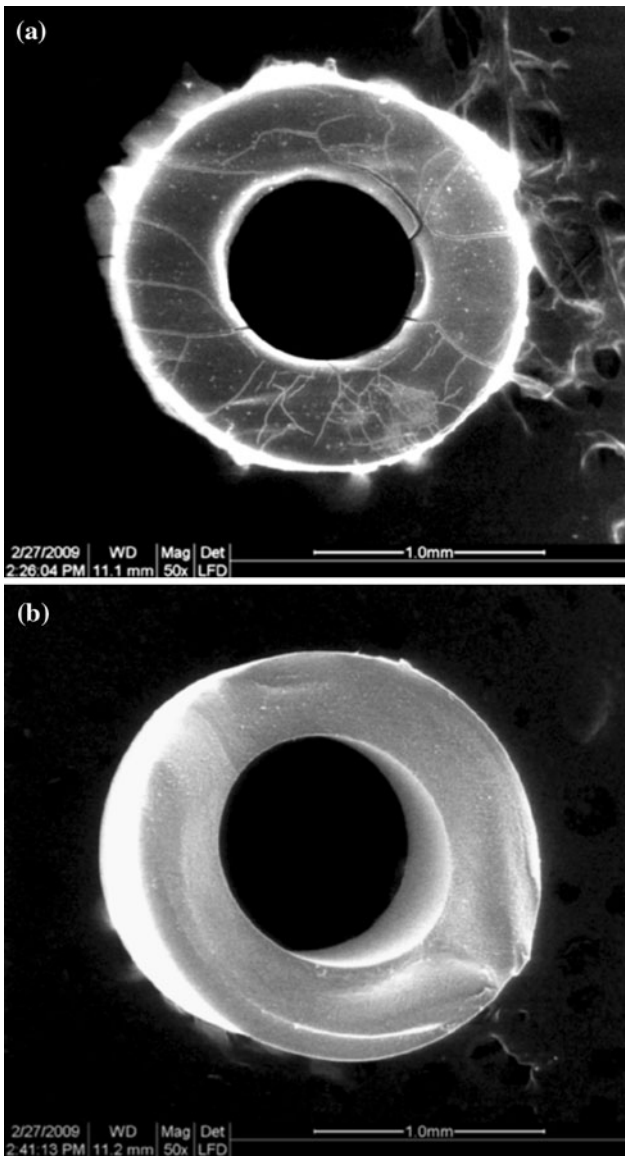

Fig. 8 Reprehensive scanning electron microscopic images of *S. aureus* accumulation on **a** PU and **b** PU/PVP-I polyurethane stents after 4 h

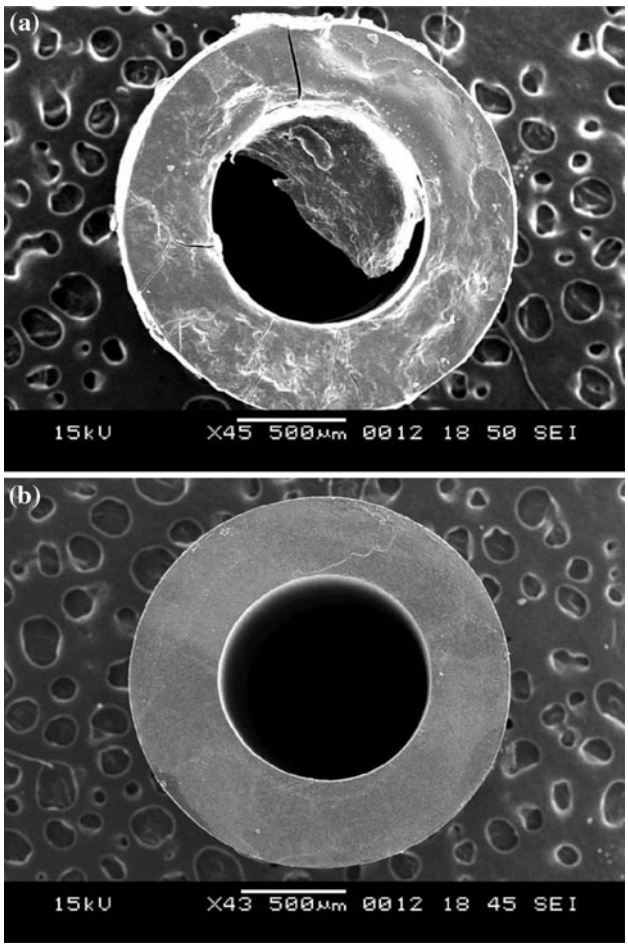

Fig. 9 Reprehensive scanning electron microscopic images of *P. aeruginosa* accumulation on **a** PU and **b** PU/PVP-I polyurethane stents after 4 h

Hydrophilic materials in addition to their advantageous properties such as lubricity and biocompatibility have also been reported to exhibit favorable resistances to both microbial adherence, the initial stage of biofilm formation, and encrustation. For example Tunney and Gorman [38] described the excellent resistance of a hydrogel coating to urinary encrustation using a dynamic in vitro model whereas several authors have described the relative resistance of hydrogels to microbial adherence in vitro [7, 16, 22, 39]. The hydrophilic antimicrobial agent employed in this study (PVP-I) was chosen for two main reasons. Firstly, being a nonantibiotic, antimicrobial agent, the possibility of developing resistance due to the local release of this agent from medical devices is lower than for conventional antibiotics [43, 44]. Secondly, there is a history for successful urological usage of PVP-I complex. For example, it has been shown that 2% PVP-I solution can be successfully used as bladder irrigation washouts for the prevention of UTI associated with intermittent urethral catheterization [45, 54, 55]. In addition to the known antimicrobial properties of PVP-I [46], this agent has been reported to possess microbial anti-adherence properties because of its hydrophilic nature, which have been reported to be potentially useful for the prophylaxis of infections. Surface entrapment modification of PVP-I on PU surface, offered the potential advantage of combining the good mechanical properties of polymers such as polyurethane with the beneficial antiadhesive and antimicrobial properties of PVP-I. The PU/PVP-I surface examined in this study was more lubricious than the bare PU surface. The good lubricity of PU/PVP-I surface is thought to arise from the reduced frictional forces (frictional coefficient)

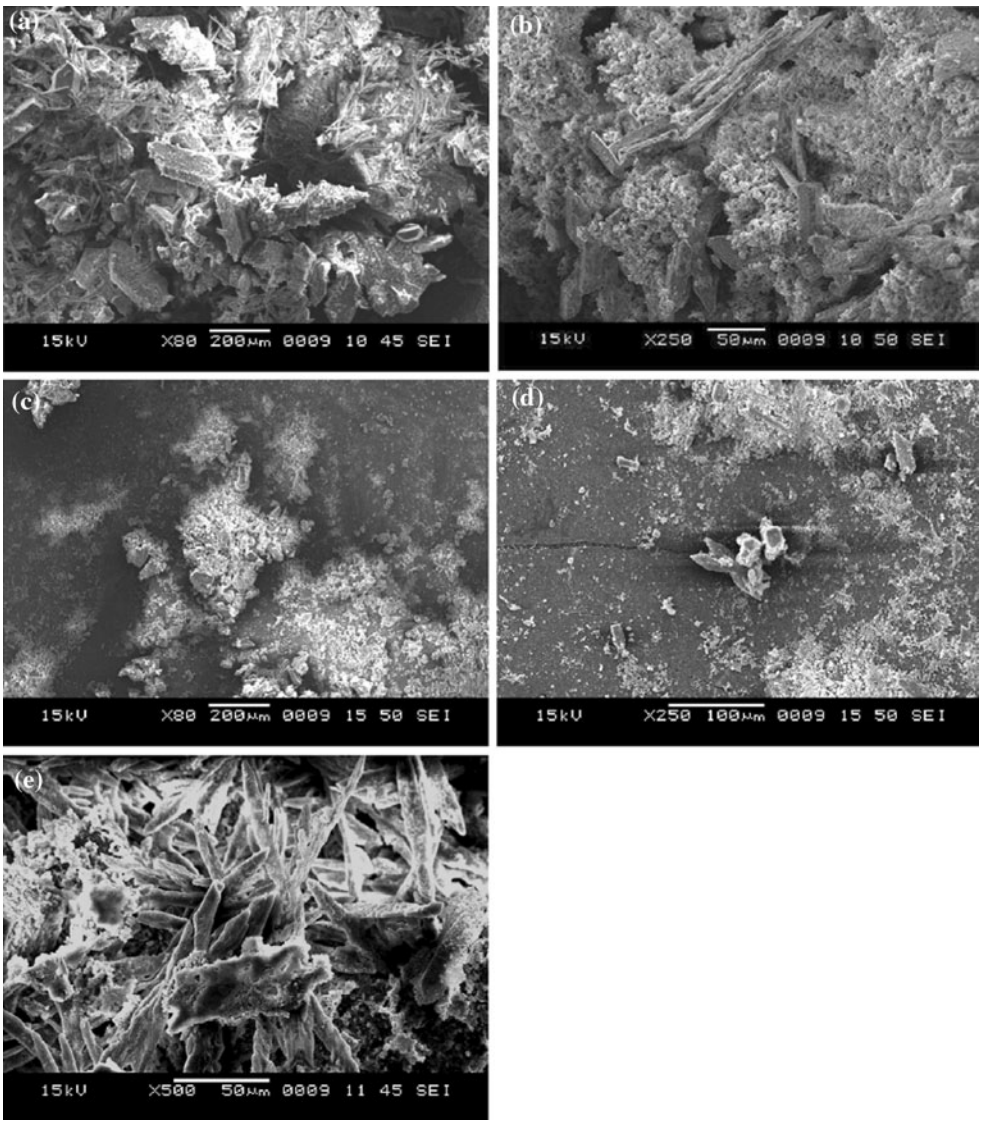

Fig. 10 Scanning electron micrographs of encrustation deposited on **a**, **b**, **e** PU; **c**, **d** PU/PVP-I surfaces after 2 weeks [**a**, **c** ×80; **b**, **d** ×250 and **e** ×500]

between the hydrated material surface and the agar/host tissue. Also, the in vitro stability analysis indicated that PU/PVP-I surface exhibited good stability because of the firm entrapment of the PVP-I molecules on the polyurethane surface.

Bacterial adhesion to biomaterial surfaces is believed to be based both on physicochemical interactions (phase one) and on molecular and cellular interactions (phase two) between bacteria and material surfaces [1, 8]. The latter is the process that bacteria adhere firmly to the biomaterial surface by the bridging function of the polymers releasing from or existing on a bacterial surface including capsules, fimbriae, and slime. Before phase two, the bacteria may attach themselves to the biomaterial surface via short- or long-range interactions (phase one) such as electrostatic attraction, van der Waals forces, hydrophobic interaction, or hydrogen. Of the physicochemical interactions, hydrophobic adsorption appears to be the most important since most bacterial surfaces contain some degree of hydrophobic moiety [10, 47, 63]. *S. aureus* and *P. aeruginosa* are the most common microorganisms involved in variety of bacterial centered infections [47]. The PU/PVP-I surface effectively reduced bacterial adhesion of gram positive *S. aureus* and gram negative *P. aeruginosa*. This adhesion to biomaterials is claimed to depend not only on the surface hydrophobicity or hydrophilicity of the biomaterial but also on the outermost bacterial cell surface structure which also plays a crucial role in bacterial adhesion to surfaces, as it interacts directly with the material surfaces. Cell-surface hydrophobicity is an important factor in the adherence and subsequent proliferation of microorganisms on solid surfaces and at interfaces [48] and the hydrophobic

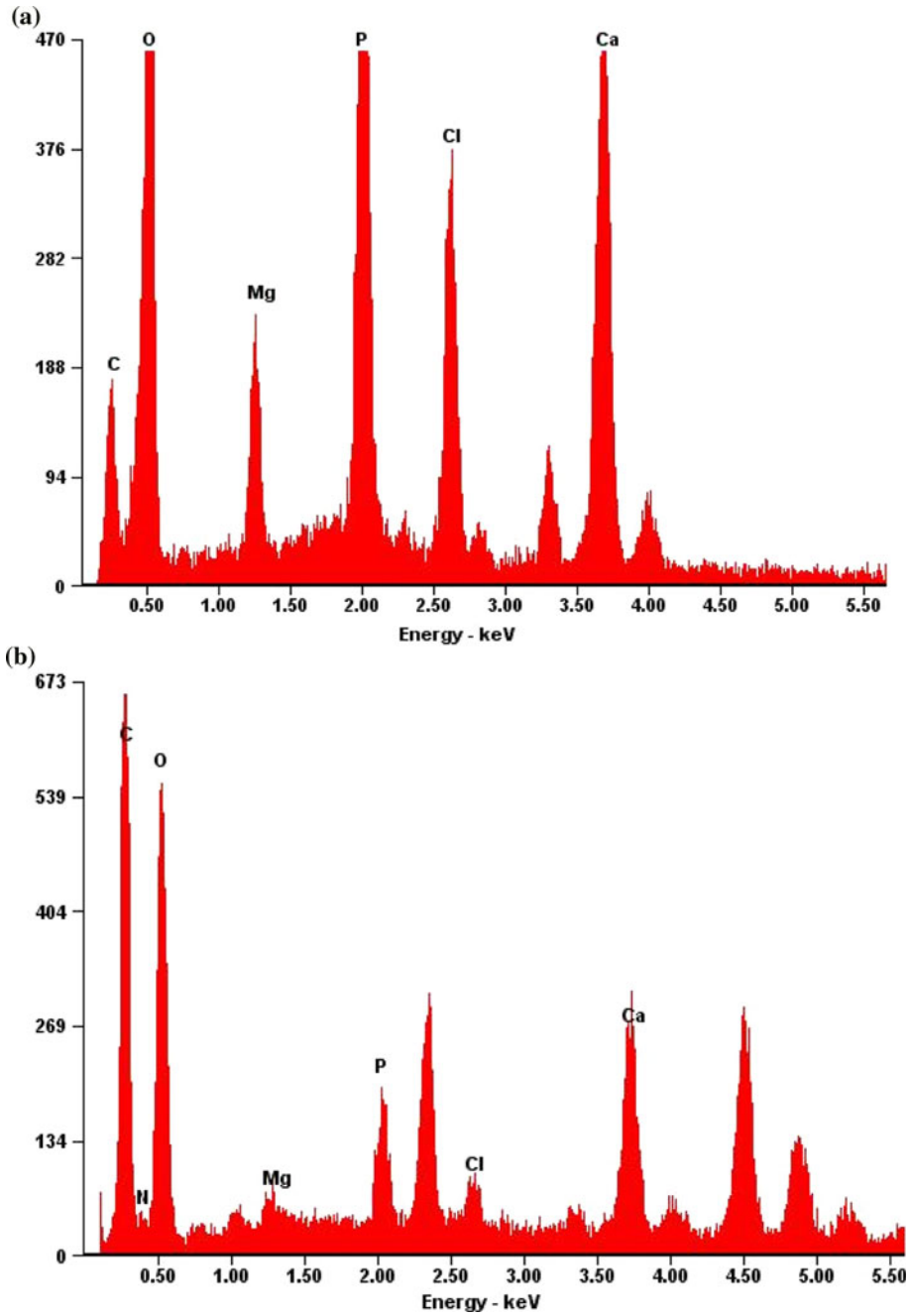

Fig. 11 EDAX counting rate of **a** PU and **b** PU/PVP-I surfaces after 1 week (168) in vitro encrustation studies

interactions have been shown to play a role in the adherence of bacteria to nonwettable plastics [49], Several studies have concluded that hydrophobicity is an important factor promoting bacterial adhesion [47, 50], this finding perfectly agrees with the present results. Herein, the bacterial adhesion level varied with the species of bacterium indicating strain variability is also one of the determinants of bacterial adhesion to materials. Indeed, *P. aeruginosa* adhesion after 4 h was greater than for *S. aureus*, this pattern has been reported previously [50]. The hydrophobicity of the organisms, as determined by the BATH test showed that *S. aureus* was more hydrophobic when compared to *P. aeruginosa* which was relatively hydrophilic in nature. These differences in cell surface hydrophobicity of the organisms may also affect their propensity to adhere to different extents to the material surfaces. It has been recognized that the antibacterial activity of the PVP-I complex is essentially attributed to the iodine ingredient, which may exist as IO^-, I^-, or I_3^- species in the aqueous media. So the effective sterilization of the PU/PVP-I film may also result from the penetration of various iodine species into the bacterial cell, and subsequently lead to halogen-induced

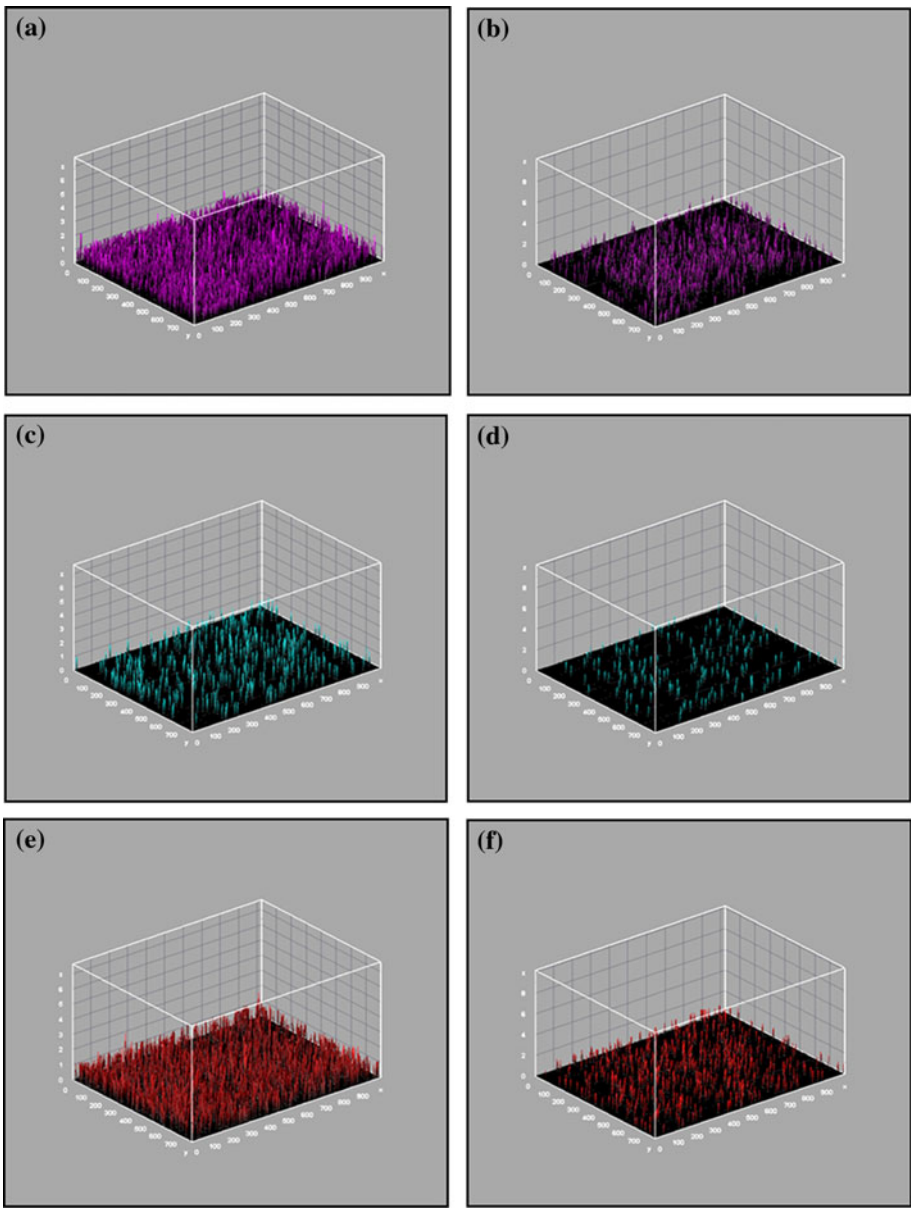

Fig. 12 Energy dispersive X-ray mapping of the major encrustation components: calcium (**a**, **b**); magnesium (**c**, **d**) and phosphorous (**e**, **f**) on PU (**a**, **c**, **e**) and PU/PVP-I (**b**, **d**, **f**) surfaces after 2 weeks

denaturation of protein and the relative enzymes, followed by the disruption of the cell membrane and leakage of the intracellular contents [45, 54–56]. Importantly, this study illustrated the ability of surface immobilized PVP-I to interfere with the microbial cell/biomaterial interactions. Therefore, it may be postulated that the enhanced performance of PU/PVP-I surface in reducing the adhesion of *S. aureus* and *P. aeruginosa* could be attributed to both the antiadherence and antimicrobial properties.

It is a known fact that the extent of encrustation on ureteral stent biomaterials is dependent, at least in part, on the surface hydrophobicity of the biomaterials [51, 52]. Hydrogels and hydrophillic polymeric materials are known to possess several properties that are advantageous for medical device applications including, lubricity, biocompatibility and resistance to infection and encrustations [51–53]. Previous studies have also reported that hydrophilic biomaterials may be more resistant to the development of encrustation in vivo. Miller et al. [64] reported that hydrogel-coated latex catheters encrusted to a lesser degree than all other catheters studied. In other studies, hydrogel-coated latex catheters were shown to be as effective at resisting encrustation in vitro as silicone and silicone elastomer-coated catheters [65, 66]. Similarly, in the present study, PU films modified with PVP-I complex were more hydrophilic and even with their nano patterned topography, were more resistant to encrustation. The deposition/distribution of struvite and hydroxyapatite crystals on the surface of PU/PVP-I showed a significant decrease as found by the fact that after 1 week of

encrustation, both the $K_{\alpha 1}$ and $K_{\beta 1}$-lines of calcium, magnesium and phosphorus were clearly resolved on PU surface, whereas the spectrum of PU/PVP-I showed no pronounced peaks, interestingly the reduction in hydroxyapatite encrustation was particularly marked. In the in vivo evaluation studies conducted by P. Hildebrandt et al. the encrustation inhibiting effect of the hydrophilic heparin coatings in biological urine was proven [61, 62]. A similar effect to the hydrophilic macromolecular coatings like PVP-I may also be assumed, when in solution, the crystallization promoting characteristics of surfaces seem to vanish if the surface is coated with these hydrophilic macromolecules. Components of the urine which adsorb on an uncoated surface will still have free growth sites which may lead to agglomeration of urine components and crystallization occurs. If the implant is covered with hydrophilic macromolecular layer, however, then components of the urine can only adsorb in a way that blocks their growth sites and prevents further crystal growth. Thus, it seems unlikely that the marginal increase in surface roughness of PU/PVP-I could have acted as nucleation sites for crystal growth and bacterial colonization as both encrustation and bacterial adherence were significantly reduced. Due to the higher crystallization potential the period of 1 week in vitro studies corresponds to a period of several months in vivo [61, 62]. Rinsing experiments with full human urine by Tunney et al. [43] showed that even after 14 days encrustation could be detected on none of the tested materials. In the current study, using artificial urine model of Tunney et al. crystal deposits were already visible after 24 h. Thus, it is clear that further work is required to better understand the differences in the physicochemical and encrustation inhibition properties of these PVP-I modified polymer surfaces.

5 Conclusion

It is demonstrated by means of ATR-FT-IR, AFM and SEM-EDAX analysis that PVP-I complex can be immobilized on Polyurethane (Tecoflex®) surface through entrapment by reversible swelling of the base polymer. Contact-angle measurements showed that modified films were highly hydrophilic in nature. SEM investigations of the entrapment structure revealed the existence of an entrapment layer of about 12–15 μm in depth. The PU/PVP-I surface showed better performance w.r.t prevention/reduction of bacterial adherence and encrustation, thereby demonstrating the success of this entrapment strategy. Thus, surface entrapment of the hydrophilic antimicrobial PVP-I complex on PU may be a promising approach in the reduction of non specific bacterial adherence and encrustation development.

Acknowledgements Anand P. Khandwekar would like to thank Council of Scientific and Industrial Research (CSIR) for providing Junior Research Fellowship (JRF) to pursue his doctoral studies.

References

1. Tunney MM, Jones DS, Gorman SP. Assessment of biofilm and related problems associated with urinary medical devices. In: Doyle RJ, editor. Methods in enzymology: biofilms, vol. 310. Florida: Academic Press; 1999. p. 558–66.
2. Gorman SP, Jones DS. Complications of urinary devices. In: Wilson M, editor. Medical implications of biofilms. Cambridge: Cambridge University Press; 2003. p. 136–70.
3. Gorman SP, Jones DS, Bonner MC, Akay M, Keane PF. Mechanical performance of polyurethane ureteral stents in vitro and ex vivo. Biomaterials. 1997;18:1379–83.
4. Gorman SP, Jones DS, Bonner MC, Akay M, Keane PF. Mechanical performance of polyurethane ureteral stents in vitro and ex vivo. Biomaterials. 1997;18(20):1379–83.
5. Zisman A, Siegel YI, Siegmann A, Lindner A. Spontaneous ureteral stent fragmentation. J Urol. 1995;153:718–21.
6. El-Sheriff A. Fracture of polyurethane double pigtail stents: an in vivo retrospective and prospective fluoroscopic study. Bri J Urol. 1995;76:108–14.
7. Tunney MM, Keane PF, Jones DS, Gorman SP. Comparison of in vitro encrustation on ureteral stent biomaterials. Biomaterials. 1996;17(15):1541–6.
8. Tunney MM, Gorman SP, Patricki S. Medical device-related infection. Revi Med Microbiol. 1996;7(4):195–210.
9. Stickler D, Ganderton L, King J, Nettleton J, Winters C. Proteus mirabilis biofilms and encrustation of ureteral stents. Urol Res. 1993;21:407–11.
10. Holmes SAV, Miller PD, Crocker PR, Kirby RS. Encrustation of intraprostatic stents—a comparative study. Br J Urol 1992;69:383–7.
11. Hedelin H, Bratt CG, Eckerdal G, Lincoln K. Relationship between urease producing bacteria, urinary pH and encrustation on indwelling urinary catheters. Br J Urol. 1991;67:527–31.
12. Squires B, Gillatt DA. Massive bladder calculus as a complication of a titanium prostatic stent. Br J Urol. 1995;75:252–3.
13. Milroy E, Chapple CR. The UroLume stent in the management of benign prostatic hyperplasia. J Urol. 1993;150:1630–5.
14. Brehmer B, Marsden PO. Route and prophylaxis of ascending bladder infection in male patients with indwelling catheter. J Urol. 1972;108:719–21.
15. Gorman SP, Jones DS. Complications of urinary devices. In: Wilson M, editor. Medical implications of biofilms. Cambridge: Cambridge University Press; 2003. p. 136–70.
16. Wironen J, Marrota J, Cohen M, Batich C. Materials used in urological devices. J Long Term Effects Med Implants. 1997;7:1–28.
17. Cox AJ, Millington RS, Hukins DWL, Sutton TM. Resistance of catheters coated with modified hydrogel to encrustation during an in vitro test. Urol Res. 1989;17:353–6.
18. Jones DS, Garvin CP, Gorman SP. Design of a simulated urethra model for the quantitative assessment of urinary catheter lubricity. J Mater Sci Mater Med. 2001;12(1):15–21.
19. Hedelin I, Grenabo L, Pettersson S. Urease induced precipitation of phosphate salts in vitro on indwelling catheters made of different materials. Urol Res. 1991;19:297–300.
20. Liedberg H, Lundeberg T. Urease induced precipitation on latex and silver coated latex in vitro. Scand J Urol Nephrol Suppl. 1991;138:239–40.

21. Gorman SP, Tunney MM, Keane PF, Van Bladel K, Bley B. Characterisation and assessment of a novel poly(ethylene oxide)/polyurethane composite hydrogel (Aquavenes) as a ureteral stent biomaterial. J Biomed Mater Res. 1998;39:642–9.
22. Kristinsson KG. Adherence of staphylococci to intravascular catheters. J Med Microbiol. 1989;28:249–57.
23. Bridgett MJ, Davies MC, Denyer SP, Eldridge PR. In vitro assessment of bacterial adhesion to hydromer-coated cerebrospinal-fluid shunts. Biomaterials. 1993;14:184–8.
24. Jansen B, Goodman LP, Ruiten D. Bacterial adherence to hydrophilic polymer-coated polyurethane stents. Gastrointest Endosc. 1993;39(5):670–3.
25. Francois P, Vaudaux P, Nurdin N, Mathieu HJ, Descouts P, Lew DP. Physical and biological effects of a surface coating procedure on polyurethane catheters. Biomaterials. 1996;17:667–78.
26. Krasovskaya SM, Uzhinova LD, Andrianova MY, Prischenko AA, Livantsov MV. Biochemical and physico-chemical aspects of biomaterial calcification. Biomaterials. 1991;12:817–20.
27. Choong SKS, Wood S, Whitfield HN. A model to quantify encrustation on ureteric stents, urethral catheters and polymers intended for urological use. BJU Int. 2000;86:414–21.
28. Khandwekar AP, Patil DP, Khandwekar V, Shouche YS, Sawant S, Doble M. TecoflexTM functionalization by curdlan and its effect on protein adsorption and bacterial and tissue cell adhesion. J Mater Sci Mater Med. 2009;20:1115–29.
29. Khandwekar AP, Patil DP, Shouche YS, Doble M. Controlling biological interactions with surface entrapment-modified polyurethane. J Med Biol Eng. 2009;29:84–91.
30. Khandwekar AP, Patil DP, Shouche YS, Doble M. The biocompatibility of sulfobetaine engineered poly(ethylene terepthalate) by surface entrapment technique. J Biomater Appl. 2010;25(2):119–43. doi:10.1177/0885328209344004.
31. Khandwekar AP, Patil DP,Shouche YS, Doble M. The biocompatibility of sulfobetaine engineered poly(methyl methacrylate) by surface entrapment technique. J Mater Sci Mater Med. 2010;21(2):635–46. doi:10.1007/s10856-009-3886-y.
32. Khandwekar AP, Patil DP, Shouche YS, Doble M. Surface engineering of poly(caprolatone) by biomacromolecules and their blood compatibility. J Biomater Appl. 2010 (in press). doi:10.1177/0885328210367442.
33. Khandwekar AP, Patil DP, Hardikar AA, Shouche YS, Doble M. In vivo modulation of foreign body response on polyurethane by surface entrapment technique. J Biomed Mater Res Part A. 2010;95A(2):413–23. doi:10.1002/jbm.a.32852.
34. Russ IG. Energy dispersive X-ray analysis on, the scanning electron microscope, In: Energy dispersive X-ray analysis, pp. 154–179, STP, 485, American Society for Testing and 154, Philadelphia; 1971.
35. Egyhazi T, Scholtz J, Beskov VS. SEM-EDAX investigations of userelated microstructural changes in an ammonia synthesis catalyst. React Kinet Catal Lett. 1984;24:1–8.
36. Glu GB, Arica MY. Surface energy components of a dye-ligand immobilized pHEMA membranes: effects of their molecular attracting forces for non-covalent interactions with IgG and HSA in aqueous media. Int J Biol Macromol. 2005;37:249–56.
37. Bhat VT, James NR, Jayakrishnan A. A photochemical method for immobilization of azidated dextran onto aminated poly(ethylene terephthalate) surfaces. Polym Int. 2007;57:124–32.
38. Bhagat PR, Pandey AK, Acharya R, Nair AGC, Rajurkar NS, Reddy AVR. Molecular iodine preconcentration and determination in aqueous samples using poly(vinylpyrrolidone) containing membranes. Talanta. 2008;74:1313–20.
39. Min XC, Ping DJ, Tai YW. Synthesis of antibacterial polypropylene film with surface immobilized polyvinylpyrrolidone-iodine complex. J Appl Polym Sci. 2005;97:2026–31.
40. Marmieri G, Pettenati M, Cassinelli C, Morra M. Evaluation of slipperiness of catheter surfaces. J Biomed Mater Res. 1996;33(1):29–33.
41. Tunney MM, Gorman SP. Evaluation of a poly(vinyl pyrollidone)-coated biomaterial for urological use. Biomaterials. 2002;23:4601–8.
42. Tunney MM, Banner MC, Keane PF, German SP. Development of a model for assessment of biomaterial encrustation in the upper urinary tract. Biomaterials. 1996;17:1025–9.
43. Ovsepyan M, Kobyakov VV, Dubrovin VI, Panov VP. Determination of polyvinylpyrrolidone in aqueous solutions by infrared spectrophotometric and spectrofluorimetric methods. Khimiko-Farmatsevticheskii Zhurnal. 1978;12:121–4.
44. Qipeng G, Jinyu H, Li Xiaoqing. Miscibility of poly(n-vinyl-2-pyrrolidone) with poly(hydroxyl ether of phenolphthalein) and polyacrylonitrile. Eur Polym J. 1996;32(4):423–6.
45. Qian X-f, Yin J, Feng S, Liu S, Zhu Z. Preparation and characterization of polyvinylpyrrolidone films containing silver sulfide nanoparticles. J Mater Chem. 2001;11:2504–6. doi:10.1039/b103708k.
46. Tunney MM, Gorman SP, Patrick S. Infection associated with prosthetic devices. Rev Med Microbiol. 1996;7(4):195–205.
47. Marshall KC. Interfaces in microbial ecology. Cambridge: Harvard University Press; 1976.
48. Rosenberg M. Bacterial adherence to polystyrene: a replica method of screening for bacterial hydrophobicity. Appl Environ Microbiol. 1981;42:375–7.
49. Gorman SP. Microbial adherence and biofilm production. In: Denyer SP, Hugo WB, editors. Mechanisms of action of chemical biocides. Oxford: Blackwell Scientific Publications Technical Services; 1991. p. 271–95.
50. Ohkafwa M, Sugata T, Sawaki M, Nakashima T, Fuse H, Hisazumi H. Bacterial and crystal adherence to the surfaces of indwelling urethral catheters. J Urol. 1990;143(4):717–21.
51. Stickler DJ, King J, Nettleton J, Winters C. The structure of urinary catheters encrusting bacterial biofilms. Cells Mater. 1993;3(3):315–20.
52. Tunney MM, Keane PF, Gorman SP. Bacterial adherence to ureteral stent biomaterials. Eur J Pharm Sci. 1996;4(Suppl 1):S177.
53. Tunney MM, Keane PF, Jones DS, Gorman SP. Comparative assessment of ureteral stent biomaterial encrustation. Biomaterials. 1996;17:1541–6.
54. Gorman SP, McCafferty DF, Woolfson AD, Jones DS. A Comparative-study of the microbial anti-adherence capacities of 3 antimicrobial agents. J Clin Pharm Ther. 1987;12(6):393–9.
55. Van den Broek PJ, Daha TJ, Mouton RP. Bladder irrigation with povidine-iodine in prevention of urinary-tract infections associated with intermittent urethral catheterisation. Lancet. 1985;1:563–5.
56. Gottardi W. The influence of the chemical behaviour of iodine on the germicidal action of disinfectant solutions containing iodine. J Hosp Infect. 1985;6:1–11.
57. Weiss E, Rosenberg M, Judes H, Rosenberg E. Cell-surface hydrophobicity of adherent oral bacteria. Curr Microbiol. 1982;7:125–8.
58. Pijanowska A, Kaczorek E, Chrzanowski, Olszanowski A. Cell hydrophobicity of Pseudomonas spp. and Bacillus spp. bacteria and hydrocarbon biodegradation in the presence of Quillaya saponin. World J Microbiol Biotechnol. 2007;23:677–82.
59. Gottenbos B, Busscher HJ, Van der Mei HC. Pathogenesis and prevention of biomaterial centered infections. J Mater Sci Mater Med. 2002;13:717–22.
60. Bruinsma GM, van der Mei HC, Busscher HJ. Bacterial adhesion to surface hydrophilic and hydrophobic contact lenses. Biomaterials. 2001;22:3217–24.

61. Hildebrandt P, Sayyad M, Rzany A, Schaldach M, Seiter H. Prevention of surface encrustation of urological implants by coating with inhibitors. Biomaterials. 2001;22:503–7.
62. Hildebrandt P, Rzany A, Bolz A, Schaldach M. Immobilisiertes Heparin als inkrustierungsresistente Beschichtung auf urologischen Implantaten. Biomed Technik. 1997;42:123–4.
63. Roberts JA, Fussell EN, Kaack MB. Bacterial adherence to urethral catheters. J Urol. 1990;144:264–9.
64. Miller JM. The effect of hydron on latex urinary catheters. J Urol. 1975;113:530.
65. Holmes S, Cheng C, Whitfield HN. The development of synthetic polymers that resist encrustation on exposure to urine. Br J Urol z992;69:651–5.
66. Cormio L. Ureteric injuries. Scand J Urol Nephrol. 1995; 171(Suppl):1–61.